

Los Alamos National Laboratory is operated by the University of California for the United States Department of Energy under contract W-7405-ENG-16

RECEIVED

MAR 13 1996

OSTI

TITLE APPLICATION OF MCNPTM TO COMPUTED TOMOGRAPHY IN MEDICINE

AUTHOR(S) Ronald C. Brockhoff
Guy P. Estes
Charles R. Hills
John J. DeMarco
Timothy D. Solberg

SUBMITTED TO American Nuclear Society 1996 Radiation Protection & Shielding Division Topical Meeting, April 21-25, 1996, No. Falmouth, Massachusetts

DISCLAIMER

This report was prepared as an account of work sponsored by an agency of the United States Government. Neither the United States Government nor any agency thereof, nor any of their employees, makes any warranty, express or implied, or assumes any legal liability or responsibility for the accuracy, completeness, or usefulness of any information, apparatus, product, or process disclosed, or represents that its use would not infringe privately owned rights. Reference herein to any specific commercial product, process, or service by trade name, trademark, manufacturer, or otherwise does not necessarily constitute or imply its endorsement, recommendation, or favoring by the United States Government or any agency thereof. The views and opinions of authors expressed herein do not necessarily state or reflect those of the United States Government or any agency thereof.

By acceptance of this article, the publisher recognizes that the U.S. Government retains a nonexclusive, royalty free license to publish or reproduce the published form of this contribution, or to allow others to do so, for U.S. Government purposes.

The Los Alamos National Laboratory requests that the publisher identify this article as work performed under the auspices of the U.S. Department of Energy.

Los Alamos Los Alamos National Laboratory
Los Alamos, New Mexico 87545

MACTED

Application of MCNPTM to Computed Tomography in Medicine

Ronald C. Brockhoff(KSU), Guy P. Estes
Charles R. Hills(mason & hanger), John J. DeMarco(ucla),
and Timothy D. Solberg(ucla)

I Introduction

The MCNPTM code has been used to simulate CT scans of the MIRD human phantom. In addition, an actual CT scan of a patient was used to create an MCNP geometry, and this geometry was computationally "CT scanned" using MCNP to reconstruct CT images. The results show that MCNP can be used to model the human body based on data obtained from CT scans and to simulate CT scans that are based on these or other models.

II Image Reconstruction Methods

Image reconstruction of a computed tomography (CT) image is based on the fact that materials of differing electron densities attenuate x-rays to varying degrees. In fact, for a beam of x-rays passing from a source to a detector, through the phantom, the total attenuation of the x-ray beam can be represented by a simple line integral as shown by Radon.^{1,2} Then, a projection of the phantom can be obtained by combining these line integrals, which for a series of parallel line integrals can be accomplished by applying a Fourier transform to the projection data at a constant projection angle. To produce such a projection a source and detector could be moved parallel to each other along opposite sides of the phantom, or a line source parallel to an array of detectors could be placed about the phantom (see Fig. 1).

Once a series of projections have been made at equal angular intervals about the phantom, they can be combined to form an image of the original phantom. Specifically, if a 1-D Fourier transform of each projection is performed, then

the image can be obtained by noting that the transform of each projection is equal to the 2-D transform of the phantom. Hence, an image of the phantom can be obtained by taking the inverse 2-D Fourier transform.³ In other words, by taking the Fourier transform of a projection, the transform along a radial line in the frequency domain of the phantom can be obtained. Thus, with an infinite number of projections and an infinite number of detectors, a complete set of data in the frequency domain can be obtained, and simple inversion will give an exact image of the phantom.

Unfortunately, only a finite number of projections and detectors can be obtained for a phantom, which only allows the construction of an approximate 2-D view of the phantom. Thus, to obtain the original image interpolation of the data in the frequency or space domain must be performed. The method of filtered backprojection was implemented to facilitate this image interpolation and reconstruction from the frequency domain. Each projection was weighted in the frequency domain to account for the discrete nature of the projections, and then backprojected into the space domain. In addition, a Hamming window was applied to reduce the occurrences of aliasing artifacts.¹

For parallel beam projections the optimum ratio between the number of projections and the number of detectors can be found via a Fourier analysis. This theoretical derivation shows that for a parallel beam geometry, the number of projections is approximately equal to $\pi/2$ times the number of detectors used in each projection.¹ For calculations in this study, 128 detectors were defined for each projection, and projection data was collected at 2 degree intervals between 0 and 360 degrees.

In essence, the image reconstruction used in

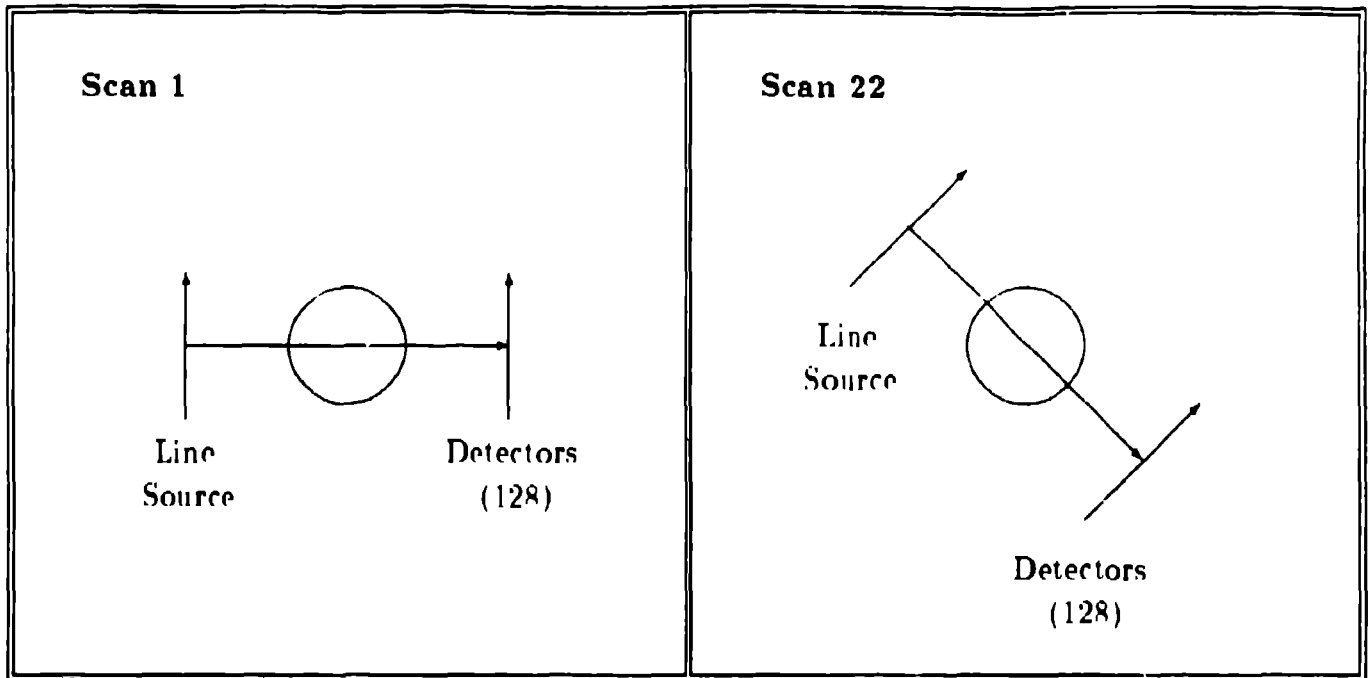


Fig. 1. A line source and a detector array are defined about the phantom and projections are calculated at 2 degree increments. The position of the source and detector arrays are shown for the 1st (i.e., 0 degrees of rotation) and 22nd (i.e., 44 degrees of rotation) scans.

this study was implemented using the VIEWIT⁴ utility, based on the following procedure: (1) the 1-D Fourier transform was applied to the projection data to convert the data to the frequency domain, (2) the data was filtered by weighting the projection data, (3) an inverse Fourier transformed to convert the data back to the space domain and (4) the filtered data was backprojected into an array in the space domain.

III MCNP Calculations

MCNP⁵ is a general-purpose Monte Carlo code for calculating the time-dependent continuous-energy transport of neutrons, photons, and/or electrons in three dimensional geometries. MCNP is used around the world for many diverse applications including nuclear criticality safety, radiation shielding, medical physics and radiotherapy, oil well logging, nuclear safeguards, and nuclear reactors, and it has been extensively benchmarked with known experimental results.^{6,7,8,9,10,11,12,13,14}

To simulate a parallel beam projection using MCNP, a line source of monodirectional x-rays

directed along a slice of the MIRDab:ab (Mathematical Internal Radiation Dosimetry) phantom was defined (see Fig. 2). The energy distribution of the source used in the calculations is shown in Fig. 3, though other energy distributions were examined. In fact, the specification of different source configurations is easily accomplished using MCNP's built-in source options. For detection purposes an array of detector volumes was defined parallel to the line source on the opposite side of the phantom. Then the phantom was rotated at 2 degree intervals using a series of surface transformations to obtain the different projections of the phantom.

The flexibility and ease of the geometry specification in MCNP allowed for the construction of several different phantoms with varying degrees of complexity. A MIRD phantom model was constructed based on published results¹⁵ as seen in Fig. 4. Then simplified phantoms based on the MIRD model were constructed with annular bones and simulated tumors. Finally, an MCNP lattice geometry of a patient's chest was constructed from an actual CT scan of the patient at UCLA.¹⁶ The original CT scan obtained

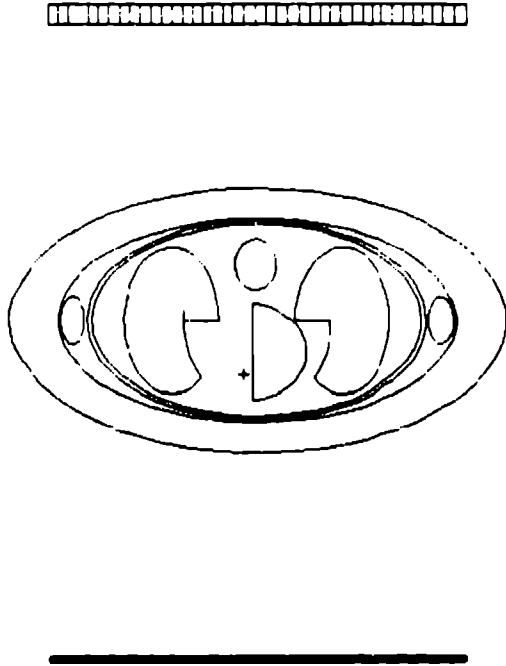


Fig. 2. MIRD geometry used for CT scanning.

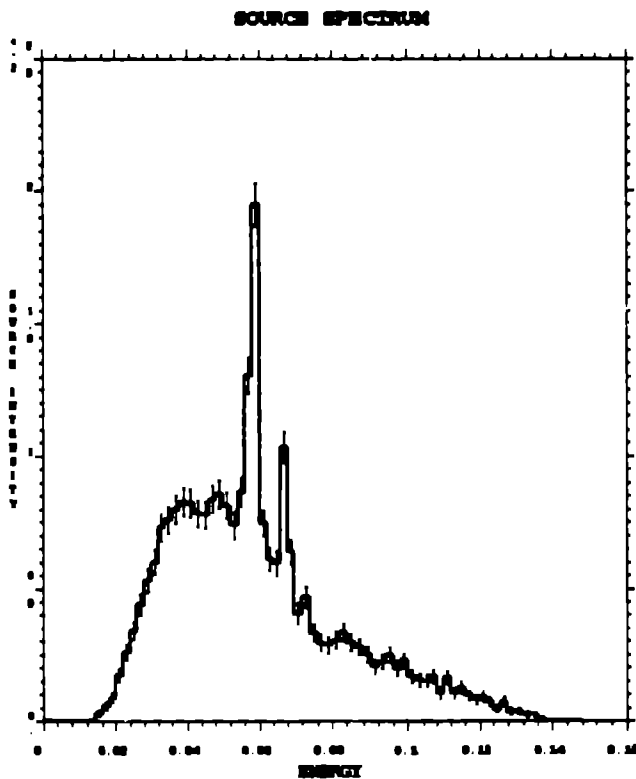


Fig. 3. Source Energy Spectrum for CT scanner.

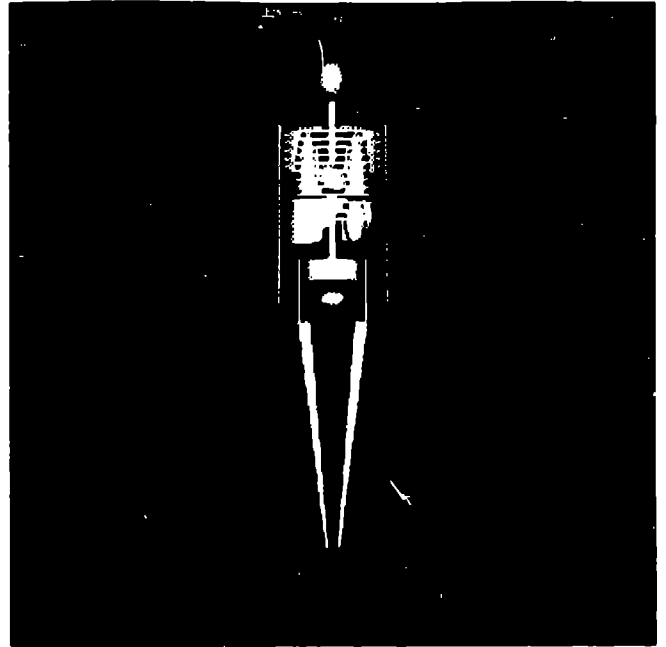


Fig. 4. An internal view of the MIRD MCNP geometry.

from UCLA is shown in Fig. 5.

To reduce the computational time required to run a simulation, the grid used to represent a slice of the phantom was reduced from the 512 X 512 grid, used in the original CT scan, to a 64 X 64 grid as shown in Figs. 6-??.

IV Results

Several MCNP simulations were performed at Los Alamos National Laboratory (LANL) to determine the quality of the CT images that could be obtained by simulating a CT scan of a phantom. The first geometry that was modeled was the MIRD phantom, and the results for a slice through the chest are shown in Fig. 7. As one can see the results are quite good for this simple geometry, and aliasing is minimal.

After the MIRD model had been successfully used to simulate a CT scan, a simplified form of the MIRD phantom was constructed. This model was constructed with hollow annular bones to represent the inhomogeneity in bone composition in the human body. The marrow was assumed to be normal MIRD flesh material. In addition, a small "tumor" was simulated in the right lung. This tumor was composed of

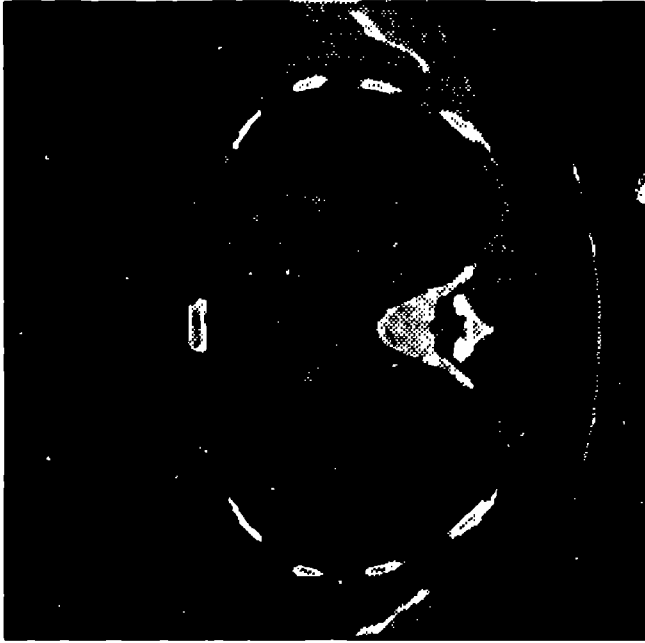


Fig. 5. UCLA CT scan of the chest with 512 X 512 resolution.

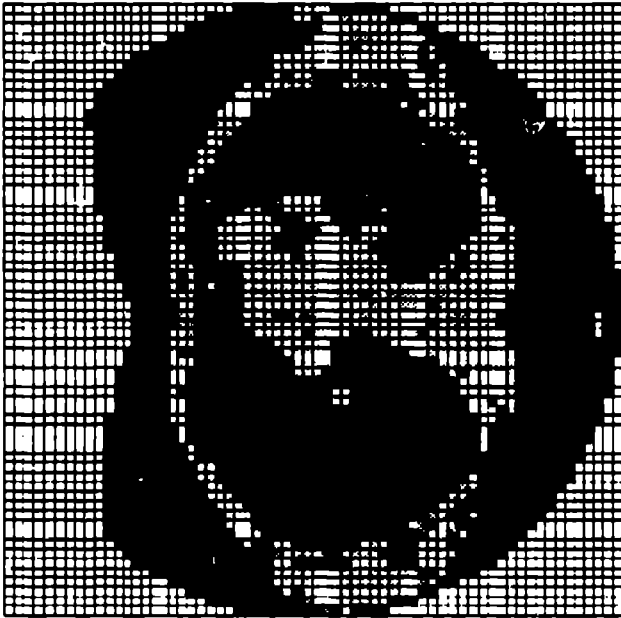


Fig. 6. UCLA MCNP geometry derived from a CT scan of the chest.



Fig. 7. Reconstructed CT of MIRD Phantom

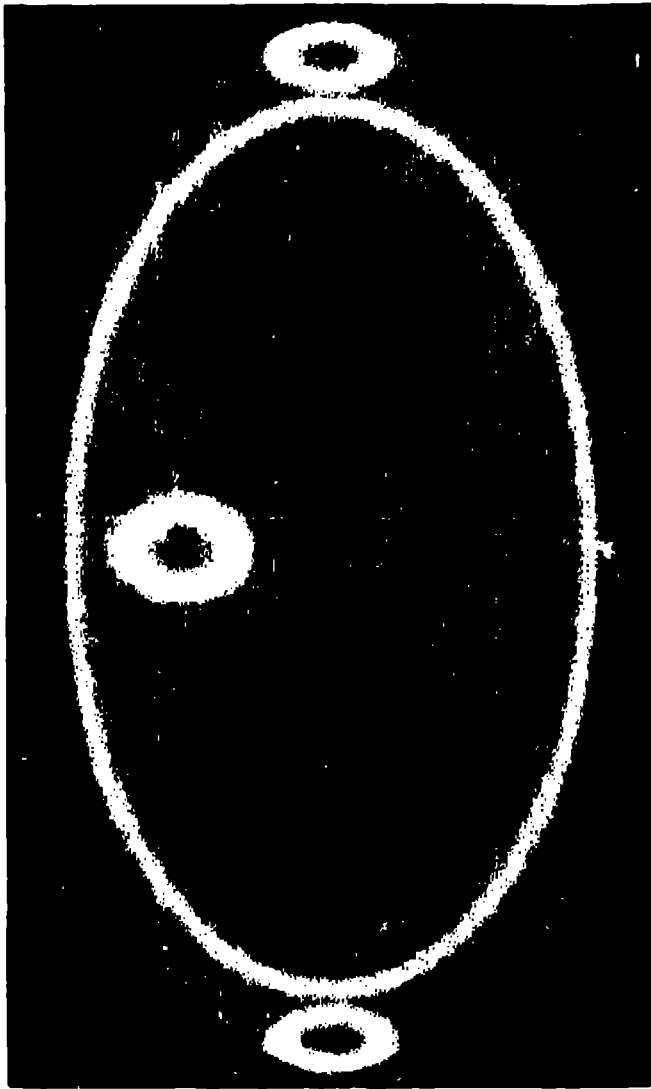


Fig. 8. Reconstructed CT of MIRDA Phantom with annular bones and a tumor in the right lung.

the same material composition as the rest of the lung, but the density was increased to 2 g/cm^3 , about twice the density of normal flesh. The results are shown in Fig. 8. The marrow inside of the bones can be clearly distinguished in the figure, and the tumor in the right lung can be seen without difficulty.

Next, the MCNP geometry obtained from a CT scan of the chest of a patient at UCLA was used to simulate the original CT scan. The results are shown in Fig. 9, and exhibit the major (as well as some minor) details of the original CT of 6. The scan is quite representative of the original scan considering the coarse grid (64×64) used in the MCNP geometry and the small

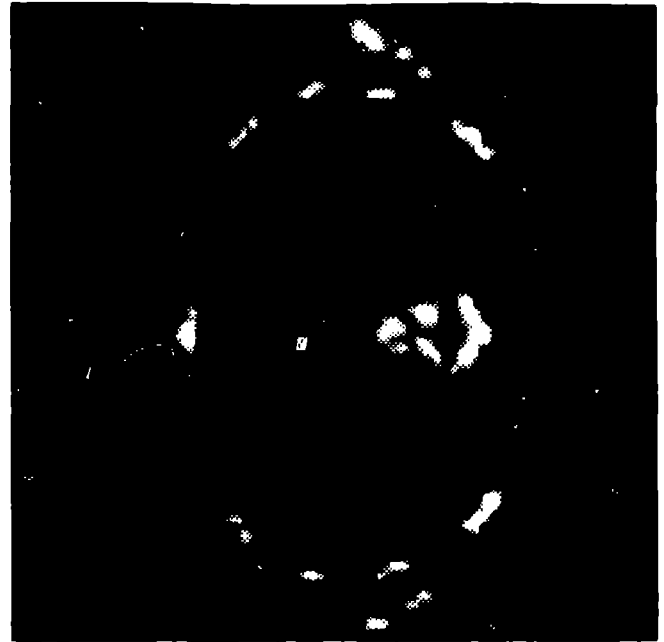


Fig. 9. Reconstructed CT of the MCNP geometry of the chest.

number of detector locations (128) used in the simulation. Further studies are planned to investigate how dose rates calculated near material interfaces with a coarse model such as this agree with those calculated in more detailed models.

Some aliasing does exist in this scan, but if the number of detectors along each projection and the number of projections were increased, then the clarity of the scan would be expected to increase.

V Conclusions

The results of this study show that MCNP can be used successfully to simulate CT scans, both for phantom geometries and for models of humans based on actual CT scans. For the latter case, the results indicate that when a geometry is constructed on a coarser spatial mesh than the original CT, the overall results of a subsequent MCNP CT reconstruction are remarkably similar to the original CT scan. This would indicate that the modeling of the human geometry in terms of a somewhat coarser spatial grid may be adequate for certain medical studies, thus reducing computer time requirements for treatment planning with detailed Monte Carlo calculations. Thus

one could conclude that such simplified MCNP geometries constructed from CT scans could be used to evaluate at least some classes of medical treatment planning scenarios. Studies are underway to perform similar calculations using a 128x128 MCNP model based on the same CT scan, and evaluate the differences in calculated dose rate for various treatment scenarios.

In addition, these studies indicate that MCNP could be used to design new CT machines, perhaps resulting in better and less costly designs for specific applications. By computationally evaluating the treatment patients receive from these machines, the machine design process could be improved. In addition, since patient-specific models of the anatomy can be implemented in MCNP, the quality of radiological procedures for each patient can be improved.

Unfortunately, the construction of CT scans from a MCNP geometry is at present computationally costly, and are not now justifiable for routine use. However, although the MCNP simulation may be computationally costly, it may be justifiable for high risk medical procedures and equipment design. The construction of accurate MCNP geometries from a CT scan can be easily implemented, and represents a potentially valuable diagnostics tool in itself.

Acknowledgments

¹ A. C. Kak and M. Slaney, *Principles of Computerized Tomographic Imaging*. (New York, NY: The Institute of Electrical and Electronics Engineers, Inc., 1988).

² J. Radon, Über die Bestimmung von Funktionen durch ihre Integralwerte längs gewissen Mannigfaltigkeiten. *Ber. Verh. Sachs. Akad. Wiss. Leipzig. Math.-Nat. Kl.*, 29, 262-279 (1917).

³ M. P. Ekstrom, Ed., *Digital Image Processing Techniques*. (New York, NY: Academic Press, Inc., 1984).

⁴ C. Potter, "Viewit User's Guide," manual as obtained via anonymous ftp from The University of Illinois at Urbana/Champaign (1990).

⁵ J. F. Briesmeister, Ed., "MCNP4A-A General Monte Carlo N-Particle Transport code," Los Alamos National Laboratory report, LA-12625-M (1993).

⁶ D. J. Whalen, D. E. Hollowell, and J. S. Hendricks, "MCNP: Photon Benchmark Problems," Los Alamos National Laboratory report LA-12196 (1991).

⁷ D. J. Whalen, D. A. Cardon, J. L. Uhle, and J. S. Hendricks, "MCNP: Neutron Benchmark Problems," Los Alamos National Laboratory report LA-12212 (1991).

⁸ J. C. Wagner, J. E. Sisolak, and G. W. McKinney, "MCNP: Criticality Safety Benchmark Problems," Los Alamos National Laboratory report LA-12415 (1992).

⁹ S. Sitaraman, "MCNP: Light Water Reactor Critical Benchmarks," General Electric Nuclear Energy report NEDO-32028 (1992).

¹⁰ C. Crawford and B. M. Palmer, "Validation of MCNP: SPERT-D and BORAX-V fuel," Westinghouse Idaho Nuclear Company, Inc. report WINCO-1112 (1992).

¹¹ C. Crawford and B. M. Palmer, "Validation of MCNP, A Comparison with SCALE, Part 1: Highly Enriched Uranium Solutions," Westinghouse Idaho Nuclear Company, Inc. report WINCO-1109 (1992).

¹² C. Crawford and B. M. Palmer, "Validation of MCNP, A Comparison with SCALE, Part 2: Highly Enriched Uranium Metal Systems," Westinghouse Idaho Nuclear Company, Inc. report WINCO-1110 (1992).

¹³ C. Crawford and B. M. Palmer, "Validation of MCNP, A Comparison with SCALE, Part 3: Highly Enriched Uranium Oxide Systems," Westinghouse Idaho Nuclear Company, Inc. report WINCO-1111 (1992).

¹⁴ A. M. Ougouag, C. A. Wemple, G. A. Rubio, and J. M. Ryskamp, "MCNP Analysis of the FOEHN Critical Experiment," Idaho National Engineering Laboratory, EG&G Idaho, Inc. ORNL/TM-12466 (1993).

¹⁵ W. S. Snyder, M. R. Ford, G. G. Warner, and S. B. Watson. "A Tabulation of Dose Equivalent per Microcurie-Day for Source and Target Organs of an Adult for Various Radionuclides." Oak Ridge National Laboratory report ORNL-5000 (1971).

¹⁶ J. Demarco, UCLA (1995).